

## Improved damage assessment of bridges using advanced signal processing techniques of CEEMDAN-EWT and Kernel PCA

Hamza Ahsan Abdullah<sup>a</sup>, Muhammad Usman Hanif<sup>b,\*</sup>, Muhammad Usman Hassan<sup>a</sup>, Janita Mahnoor Shahid<sup>a</sup>, Shaukat Ali Khan<sup>a</sup>, Ather Ali<sup>a</sup>

<sup>a</sup> School of Civil and Environmental Engineering (SCEE), National University of Sciences and Technology, H-12, Islamabad, Pakistan

<sup>b</sup> SDU.Structures, Civil and Architectural Engineering, Department of Technology and Innovation, University of Southern Denmark, 5230 Odense, Denmark



### ARTICLE INFO

**Keywords:**

Structural Health Monitoring (SHM)  
Damage Detection  
Signal Processing  
CEEMDAN  
EWT  
Kernel PCA and Performance metrics

### ABSTRACT

Bridges are subjected to a variety of loads throughout their service life, including service loads, seismic events, and environmental forces, which may compromise their structural integrity. As these structures are significant and expensive assets, there is a growing emphasis on using advanced structural health monitoring (SHM) techniques to ensure their safety and longevity. This research introduces a refined approach for the precise detection of damage in bridges using state-of-the-art signal processing methods. In the initial phase, ambient vibration data are captured via accelerometers strategically installed on the bridge to record its response in healthy state for baseline data. Vibration data are then processed using Complete Ensemble Empirical Mode Decomposition with Adaptive Noise (CEEMDAN) to extract intrinsic mode functions (IMFs). These IMFs are used for signal reconstruction followed by further analysis thorough Empirical Wavelet Transform (EWT). This combination efficiently segregates the bridge vibrations into distinct modes, thereby enhancing the identification of potential damage by mitigating noise interference and closely spaced frequencies. The spectral centroids (SC) of these modes are computed using Short-Time Fourier Transform (STFT) to serve as critical damage-sensitive features. Subsequently, an artificial intelligence model utilizing Kernel Principal Component Analysis (KPCA) is employed. This model is trained on baseline data to establish control limits and then used to detect deviations in new datasets by analyzing changes in the Squared Prediction Error (SPE) and Hotelling's  $T^2$  statistic, it enables effective damage detection. The efficacy of this methodology is empirically validated using real-world data collected from the Z-24 bridge, demonstrating its practical applicability and reliability. Additionally, the health condition of an RC bridge was also monitored to detect any potential damage. Overall, the innovative integration of CEEMDAN, EWT, and KPCA in this research offers a robust framework for early damage detection, promising significant improvements in the maintenance and monitoring of bridge structures, the efficiency of which was validated through performance metrics.

### 1. Introduction

The health, safety and reliability of civil infrastructures, particularly bridges, hold paramount significance and play a fundamental role in sustainable development. Bridges play a vital role in significantly reducing travel time and conserving the transportation costs, thus contributing to a country's prosperity [1–4]. However, the operational and environmental loads that bridges experience throughout their service life expose them to various risks entailing potential damage, necessitating effective risk assessment and monitoring of their health and behavior, prompting mitigating measures [5]. Monitoring the

behavior of the system periodically is, therefore, indispensable to identify and address damage in its early stages [6]. Structural health monitoring (SHM) techniques have gained popularity in recent decades for monitoring purposes due to their advantages over traditional visual inspection methods which have proven to be laborious, time-consuming, and subjective [5,7]. SHM involves damage assessment using characteristics sensitive to damage which are derived from sensors attached to the structures. This makes the damage assessment efficient, cost-effective and economical in terms of human resources [8–11].

Different researchers have interpreted data from SHM systems using different techniques to monitor the condition of the structure by setting

\* Corresponding author.

E-mail address: [muha@iti.sdu.dk](mailto:muha@iti.sdu.dk) (M.U. Hanif).

priorities for safety. Traditionally, the interpreted data are monitored using either a model-based or data driven method. The model-based approach builds a finite element model for damage identification based on the structure's modal parameters. In data driven method, the data acquired using sensors are monitored to detect anomalies that indicate damage [7]. In modern-day research, vibration-based data-driven methods are acutely used in the field of SHM for damage detection with the foundational role of feature extraction and pattern recognition for accurate and efficient damage-sensitive features extraction [8]. As a result, these feature extraction approaches for damage detection require special attention, and the prevalent practice has been to use signal processing methods such as the Short-Time Fourier Transform (STFT) and the Wavelet transform (WT). These methods provide insights on structural properties and integrity by keeping in view the nonlinear nature of signals. However, despite these improvements, challenges prevail in these methods. STFT confronts snags in representing instantaneous frequencies with the desired resolution, and WT encounters challenges in decomposing time signals and computing instantaneous frequencies due to the intrinsic incompatibility of the prescribed basis of WT with the analyzed signal [8, 9].

A recent development in the field of adaptive mode decomposition techniques has overcome the limitations of traditional methods by introducing efficient data-driven approaches designed to process complex data for structural damage identification. Over the preceding decade, Empirical Mode Decomposition (EMD) has gained significant attention, because of its ability to deal with non-stationary and nonlinear signals, making this method suitable for application on real-world data [10]. To identify the location of the damage, Obrian et al., [11] applied EMD to break down the signal into Intrinsic Mode Functions (IMFs) related to the vehicle speed component as a damage sensitive feature. However, the dependence on a single IMF and the frequent occurrence of mode mixing brought on by signal intermittency have negatively impacted the EMD. An improved method developed by Wu and Huang [12], named as Ensemble Empirical Mode Decomposition (EEMD) enhances signal analysis in noisy, non-linear, and non-stationary environments by addressing the mode mixing issue of EMD through white noise addition, enabling better scale separation, and reducing computational challenges. Both techniques, EMD and EEMD, have been widely used to assess damage in civil structures [13–15]. To extract damage-sensitive features, Entezami et al., [16] provide a unique feature extraction method that combines a correlation-based dynamic temporal warping algorithm with a hybrid EEMD-ARARX algorithm for SHM. Although EEMD overcomes some of the drawbacks of EMD, its extreme sensitivity to the amplitude of the introduced noise and environmental factors makes signal reconstruction inaccurate.

To achieve accurate mode extraction and better spectral separation, Torres et al. [17] provided an improved EEMD with Adaptive Noise (EEMD-AN) method. This method involved adding a certain noise level to EEMD at each stage of the decomposition process. Although EEMD-AN partly overwhelms the limitations of EMD and EEMD, yet it fails to rebuild the signal effectively because it is highly affected by the magnitude of the noise add-ons. [18]. To tackle all these issues in EMD and its variant, Torres et al. [19] proposed Complete Ensemble Empirical Mode Decomposition with Adaptive Noise (CEEMDAN), which strives for precise signal reconstruction with improved spectral separation of modes and reduced processing cost. This adaptation reduced the variability in mode generation and the influence of added noise, offering a more efficient and accurate approach to signal decomposition. However, this method is still susceptible to mode mixing issue [20].

Another paramount adaptive signal decomposition method for system identification, signal processing, and evaluating structural damage, is the Empirical Wavelet Transform (EWT) method [21–23]. Gilles et al. [24] introduced the Empirical Wavelet Transform (EWT), advancing signal analysis by developing adaptive wavelets from signal-specific Fourier supports, enhancing mode separation and computational

efficiency. Xia and Zhou et al., [25] used EWT for condition assessment in civil structures, focusing on mono-component feature extraction, which overcame EMD issues of mode separation and computational efficiency. Mousavi et al. [9] proposed an innovative EWT-ANN approach for damage detection and localization in steel truss bridges, efficiently distinguishing between healthy and damaged states under varied excitations, demonstrating the approach's effectiveness in identifying damage locations and severity. However, EWT is also susceptible to noisy data, as noise can lead to inappropriate frequency segment separation, especially when data have overlapping segments in the Fourier spectrum due to environmental noise, which necessitates the need for data cleaning before segmentation [26].

Furthermore, artificial intelligence, including Convolutional Neural Networks (CNN), Support Vector Machine algorithm (SVM), and fuzzy logic algorithm are extensively used nowadays to process data and automate detection, by addressing the limitations of the previous methods [27–29]. Pan et al. [30] provided a data-driven methodology framework for damage detection, that combined SVM with improved feature extraction methods including Teager-Huang transform (THT), Hilbert-Huang transform (HHT), and wavelet transform. Marinello et al. [31] introduced a decision tree ensemble (DTE) method for structural damage detection and localization by dynamic property analysis of vibration data. Alazzawi and Wang [32] developed an innovative SHM method using the Deep Residual Network (DRN) algorithm to analyze acceleration responses from structures subjected to ambient vibrations.

Chen et al. [33] used a unique approach to detect structural degradation that combined the Continuous Wavelet Transform (CWT) with a Deep Convolutional Neural Network (DCNN). Gu et al. [34] described an improved methodology for structural damage detection that combines Sparse Component Analysis (SCA) and Blind Source Separation (BSS) for output-only modal identification, which is critical for monitoring the health of large-scale structures. However, potential drawbacks may arise from the complexity of implementing such advanced signal processing techniques, the reliance on precise time-frequency transformation that could be susceptible to signal noise, and the risk of over-fitting during the clustering process, especially with noisy or limited datasets.

Sen et al. [35] discussed using Principal Component Analysis (PCA) to detect structural damage in bridge structures by identifying sudden discontinuities in principal components. The limitations of PCA in detecting nonlinear behavior, emphasize the use of kernel functions for better handling of nonlinearity. KPCA addresses the shortcomings of PCA by generating nonlinear subspaces, thus enhancing the capability to identify damages in such systems [36]. Bisheh and Amiri [8] introduced a novel methodology for structural damage detection that combined Variational Mode Decomposition (VMD) and Kernel Principal Component Analysis (KPCA), aimed at overcoming environmental and operational influences. This method efficiently processed vibration data to extract damage-sensitive features, demonstrating better accuracy in identifying structural damage across various scenarios.

Despite the progression in contemporary signal processing methods, especially for SHM, these methods encounter numerous snags. One of the major hurdles is their sensitivity to noise and environmental variations, thus negatively affecting the accuracy of the damage assessment. Customary frequency-based methods, such as the Discrete Fourier Transform (DFT), strive with non-linear and non-stationary signals, restraining their effectiveness in real-world applications. Additionally, time-frequency methods often suffer from mode mixing, which shrouds the true nature of signal components. The requirement of predefined parameters is also subjective and is likely to manipulate the accuracy. Furthermore, time-domain techniques stereotypically necessitate data from all degrees of freedom, making them complex and prone to errors [37]. The incidence of closely spaced modes and noisy signals further hampers the reliability of these methods. All these dynamics call for the alternate modes and means beyond existing methods, which may have relatively more accuracy, reliability and economy.

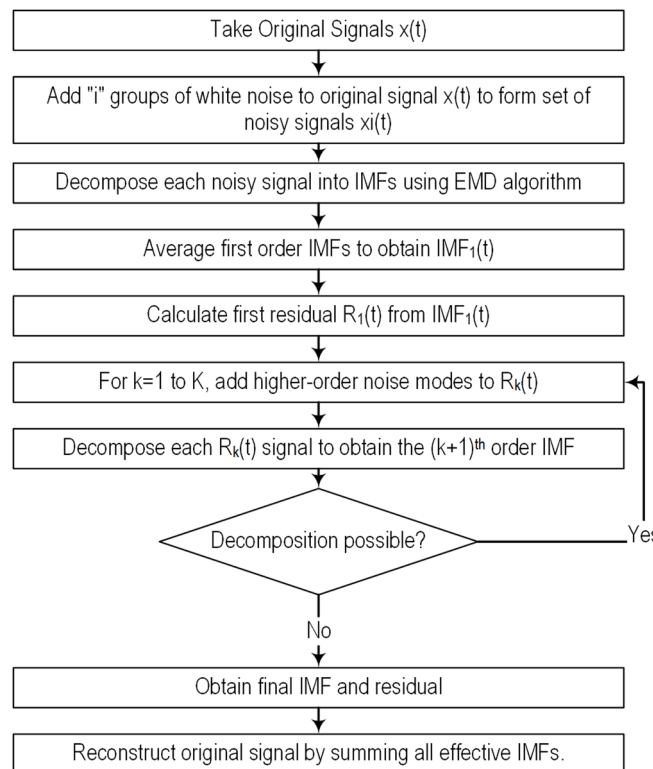


**Fig. 1.** Flowchart of CEEMDAN.

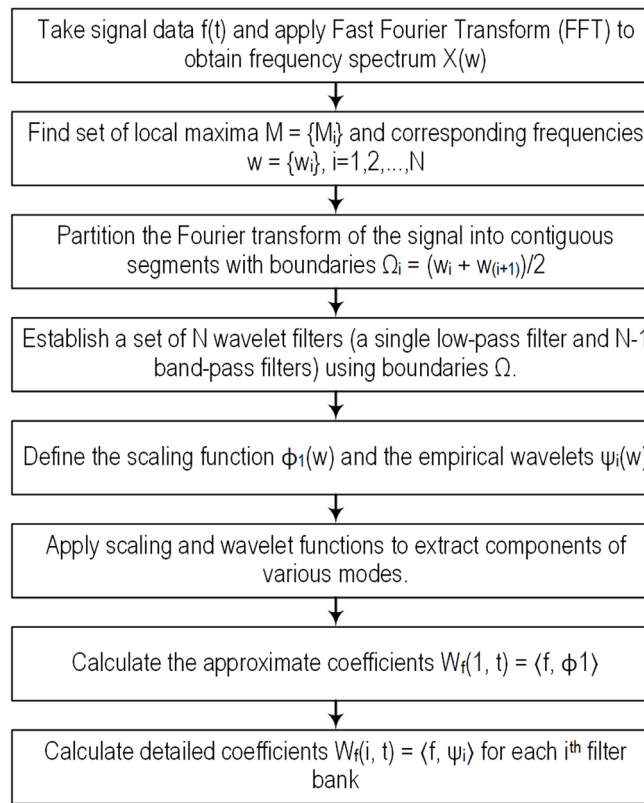
Based on the comprehensive literature review, this study aims to propose an innovative automated, data-driven method for detecting structural damage. It intends to address previous limitations in bridge damage detection by combining the benefits of CEEMDAN, EWT, and KPCA. This study addresses a significant gap in SHM, which is the challenge of precisely identifying structural damages from complex, noisy, non-linear and non-stationary data, a constraint that existing methods often encounter due to their limited ability to differentiate between environmental noise and actual signs of structural issues. This research integrates advanced signal processing techniques including CEEMDAN, EWT, and KPCA into a comprehensive framework for better signal decomposition and feature extraction and develops robust damage detection methods that are less sensitive to noise and environmental variations to enhance accuracy and reliability. The proposed framework was validated through comprehensive experimental study of Z-24 bridge and a newly constructed reinforced concrete (RC) prototype bridge, aiming to establish its effectiveness in real-world scenarios. By offering a more refined analysis and feature extraction process, the proposed approach aims to significantly enhance the precision and reliability of damage detection in bridge structures. This research also addresses the mode mixing issue of the CEEMDAN method and EWT susceptibility to noise by reconstructing the decomposed signals and further decompose the reconstructed signals using EWT, giving a detailed overview of the damage sensitive features in acceleration data. This research is innovative due to its integration of CEEMDAN, EWT, and KPCA, which collectively captures the nonlinear and non-stationary properties of vibration signals. This approach extracts key features critical for detecting damage, surpassing the constraints of earlier methods that rely on linear assumptions or single decomposition techniques.

There are five main steps involved to implement the proposed methodology: (1) signal pre-processing using CEEMDAN which give IMFs by decomposing the vibration signals; (2) reconstruction of the signals using effective IMFs based on the correlation coefficient and kurtosis values of IMFs; (3) decomposition of reconstructed signals using EWT; (4) feature extraction using STFT to obtain the spectral sub-band

features specifically the spectral centroids of the IMFs; and, (5) damage classification using KPCA, including the dimensionality reductions of the features and enhancement in the distinction of the damage states. The methodology was evaluated through metric performance, by comparing its results with EMD-KPCA and EWT-KPCA. This initial step is advantageous over conventional methods due to CEEMDAN's ability to effectively handle non-linear and non-stationary signals, ensuring a more accurate representation of structural responses. Then the reconstructed signals undergo spectral analysis through EWT, offering a distinctive advantage in capturing high-resolution spectral properties of each mode. EWT's efficiency in decomposing non-linear and non-stationary signals surpasses traditional techniques such as Fast Fourier Transform (FFT), enabling more nuanced analysis. A feature extraction step was performed on each EWT decomposed mode, where STFT analysis was utilized to extract the spectral centroid of each mode. This step contributes to the construction of a feature matrix that selectively retains damage-relevant information, ensuring a focused dataset for further analysis. The last step is to project the created matrix into a KPCA model, resulting in a compact representation of the data.  $T^2$  and SPE statistics are damage-sensitive features that aid in the identification of structural damage by identifying rapid changes in control charts. Experimental validation on the Z-24 bridge and prototype RC bridge demonstrates the suggested method's ability to reliably detect structural degradation. This methodology outperforms the existing methodologies by efficiently lowering the impact of operational and environmental elements while also limiting false alarms, establishing itself as a reliable option for structural health monitoring.

## 2. Damage detection using advanced signal processing

This study presents a novel approach to damage detection that employs CEEMDAN, EWT, and KPCA. Initially, a comprehensive theory for the methods used in proposed methodology is presented. Then, detailed methodology for damage detection is described and implemented on a real-life bridge to evaluate its effectiveness. Lastly, we evaluate the

**Fig. 2.** Flowchart of EWT.

efficiency and accuracy of our method by comparing it with existing approaches through performance evaluation metrics.

### 2.1. Theoretical fundamentals

#### 2.1.1. Complete ensemble empirical mode decomposition with adaptive noise (CEEMDAN)

Torres et al. [38] created CEEMDAN, an adaptive signal processing approach that improved signal decomposition using EEMD. This approach addresses concerns such as mode mixing, residual noise in Intrinsic Mode Functions (IMFs), and the difficulty in averaging IMFs with different numbers produced by introducing varying white Gaussian noise in EEMD [39]. CEEMDAN generates IMFs by introducing white noise adaptively at each decomposition stage and computing only the residuals. The cumulative effect of adding white noise across stages balances out, reducing reconstruction errors, enhancing decomposition accuracy, and minimizing mode mixing [40].

Let  $x(t)$  be the original signals and  $w^i(t)$  be  $i^{\text{th}}$  Gaussian white noise with  $N(0,1)$ . And the  $j^{\text{th}}$  mode IMFs from EMD are produced by the operator  $E_j(\cdot)$  for a given signal. So, the algorithm of CEEMDAN is as follows [38–40]:

- (i) First, “ $i$ ” group of white noise are generated and added to the original signals  $x(t)$  resulting in creation of “ $i$ ” group of noisy signals,  $x_i(t)$ , where the  $i^{\text{th}}$  set of noisy signals are represented as follows:

$$x_i(t) = x(t) + \epsilon_0 w^i(t) \quad (1)$$

where,  $\epsilon_0$  represents the amplitude of the  $i^{\text{th}}$  white noise added and  $i = 1, 2, \dots, I$ .

- (ii) In the second step, decomposed the above set of noisy signals into IMF using EMD algorithm. And average the first-order IMFs derived from decomposing each set of noisy signals using the

EMD algorithm, to get the first-order IMF of the signal  $x(t)$ , denoted as  $\overline{\text{IMF}}_1(t)$ , and it can be represented as follows:

$$\overline{\text{IMF}}_1(t) = \frac{1}{I} \sum_{i=1}^I \text{IMF}_1^i(t) \quad (2)$$

where,  $\text{IMF}_1^i(t)$  represents the first IMF derived from  $i^{\text{th}}$  decomposed noisy signals

- (iii) In third step, calculate the first residual ( $R_1(t)$ ) from the above IMF, as follows:

$$R_1(t) = x(t) - \overline{\text{IMF}}_1(t) \quad (3)$$

- (iv) Now after obtaining the first IMF,  $i$  group of signals are constructed by adding modes in remaining signals as  $R_1(t) + \epsilon_1 E_1(w^i(t))$ , ( $i = 1, 2, \dots, I$ ). Then EMD algorithm is used to decompose each  $i$ -group signal individually. Then obtain the integrated average, which is like step 1. This will result in second order IMF, which is denoted as  $\overline{\text{IMF}}_2(t)$ , the process for  $i = 1, 2, \dots, I$ , is as follows:

$$\overline{\text{IMF}}_2(t) = \frac{1}{I} \sum_{i=1}^I E_1(R_1(t) + \epsilon_1 E_1(w^i(t))) \quad (4)$$

- (v) Now for  $k = 2, 3, \dots, K$ , the  $k$ -th residue  $R_k(t)$  are calculated as follows:

$$R_k(t) = R_{k-1}(t) - \overline{\text{IMF}}_k(t) \quad (5)$$

- (vi) Again, decompose the signal  $R_k(t) + \epsilon_k E_k(w^i(t))$ , ( $i = 1, 2, \dots, I$ ) to obtain the  $(k+1)$  th-order IMF, which is similar to step 1 and step 4. The result is recorded as  $\overline{\text{IMF}}_{(k+1)}(t)$ , as follows:

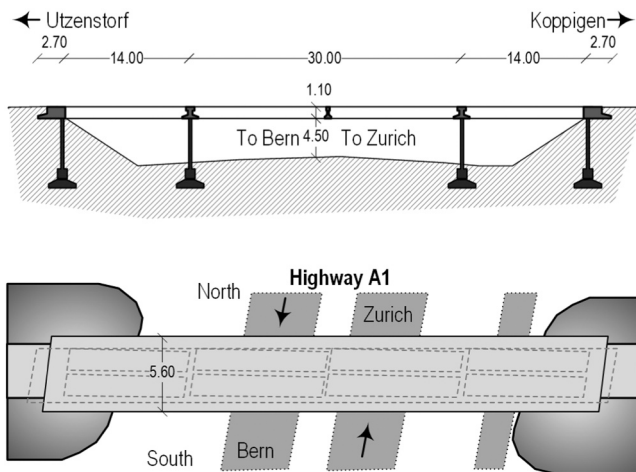


**Fig. 3.** Front view (shown in top) and top view (shown in bottom) of the Z24 bridge, reproduced from [53].

$$\overline{\text{IMF}}_{(k+1)}(t) = \frac{1}{I} \sum_{i=1}^I E_1(R_k(t) + \epsilon_k E_k(w^i(t))) \quad (6)$$

(vii) This iterative process progresses systematically, where each  $k^{\text{th}}$  residue,  $R_k(t)$ , serves as the basis for generating the  $(k + 1)^{\text{th}}$  IMF. The decomposition of the residual proceed further until there is no longer feasible, typically reaching a point where in residual at most one extreme value is remaining. This last IMF becomes the  $k^{\text{th}}$  IMF, which is denoted as  $\overline{\text{IMF}}_k(t)$ , and the final residue ( $Fr(t)$ ), which can be represented as:

$$Fr(t) = x(t) - \sum_{k=1}^K \overline{\text{IMF}}_k(t) \quad (7)$$

(viii) The original signal  $x(t)$  can be reconstructed by adding all IMF and residual, expressed as follows:

$$x(t) = \sum_{k=1}^K \overline{\text{IMF}}_k(t) + Fr(t) \quad (8)$$

It is noted that the  $\epsilon_i$  coefficients obtain at each stage allow to select the signal-to-noise ratio (SNR). The flowchart of procedure of CEEMDAN are shown in Fig. 1.

### 2.1.2. Empirical wavelet transform

The Empirical Wavelet Transform (EWT) introduces a novel approach for adaptively decomposing signals, focusing on their contained information, was introduced by Gilles [41]. Unlike traditional methods, EWT constructs a wavelet filter bank dynamically, extracting various signal modes by segmenting its Fourier spectrum. This adaptive basis, tailored to the signal itself, enables a comprehensive analysis of both stationary and non-stationary components. The EWT addresses the theoretical foundation gap found in methods, such as Empirical Mode Decomposition (EMD), by offering a mathematical framework for its adaptive filtering process. Through experiments on simulated and real signals, EWT demonstrates its effectiveness in capturing essential signal characteristics. The adaptive nature of EWT estimates frequency components and computes boundaries to extract oscillatory components. The method includes procedures such as performing the Fast Fourier Transform (FFT), detecting maxima in the Fourier spectrum, segmenting the spectrum, and defining boundaries. By creating a bank of wavelet filters based on these boundaries, EWT surpasses the standard Continuous Wavelet Transform (CWT) in terms of resolution for retrieving geological and stratigraphic information. This method has been previously applied in a variety of domains, including structural health monitoring, signal and image processing, power system signal analysis and disease detection. One of the most significant benefits of the method is its ability to successfully handle nonlinear and non-stationary signals. In order to implement the EWT on the signals, following procedure will be followed [42–44]:

- First take the signals data  $f(t)$  on which EWT need to be applied and apply fast Fourier transform (FFT) to obtain the frequency spectrum  $X(w)$ .
- From the frequency spectrum find the set of local maxima  $M$ , represented as  $M = \{M_i\}_{i=1,2,\dots,N}$ , and calculate their corresponding frequencies  $w = \{w_i\}_{i=1,2,\dots,N}$ . Here,  $N$  represent the total number of maxima obtain from the Fourier spectrum.
- The Fourier transform of the signal is then partitioned into contiguous segments, with boundaries  $\Omega_i$ , identified based on the center of consecutive local maxima of the spectrum, as:

$$\Omega_i = \frac{w_i + w_{i+1}}{2} \quad (9)$$

where  $w_i$  and  $w_{i+1}$  are two consecutive frequencies with the set of boundaries is  $\Omega = \{\Omega_i\}_{i=1,2,\dots,N-1}$ .

- Establish a set of  $N$  wavelet filters, comprising a single low-pass filter and  $N-1$  band-pass filters, determined by the specified boundaries. The mathematical representation of the scaling function  $\phi_1(w)$  and the empirical wavelets  $\psi_i(w)$  of the Fourier spectrum are given by:

$$\phi_1 = \begin{cases} 1, & |\omega| \leq (1 - \gamma)\Omega_1 \\ \cos\left(\frac{\pi}{2}\beta((1/2\gamma\Omega_i)(|\omega| - (1 - \gamma)\Omega_i))\right) & (1 - \gamma)\Omega_1 < |\omega| \leq (1 + \gamma)\Omega_1 \\ 0, & \text{otherwise} \end{cases} \quad (10)$$

$$\psi_i = \begin{cases} 1 & (1 + \gamma)\Omega_i < |\omega| < (1 - \gamma)\Omega_{i+1} \\ \cos\left(\frac{\pi}{2}\beta((1/2\gamma\Omega_{i+1})(|\omega| - (1 - \gamma)\Omega_{i+1}))\right) & (1 - \gamma)\Omega_{i+1} \leq |\omega| \leq (1 + \gamma)\Omega_{i+1} \\ \sin\left(\frac{\pi}{2}\beta((1/2\gamma\Omega_i)(|\omega| - (1 - \gamma)\Omega_i))\right) & (1 - \gamma)\Omega_i \leq |\omega| \leq (1 + \gamma)\Omega_i \\ 0, & \text{otherwise} \end{cases} \quad (11)$$

where,  $\gamma$  is introduced to avoid the overlapping between the two consecutive transitions, and  $\beta(x)$  is defined as an arbitrary function represented as follows:

$$\beta(x) = \begin{cases} 0, & \text{if } x \leq 0 \\ 1, & \text{if } x \geq 1 \\ \beta(x) + \beta(1-x) = 1, & \text{if } x \in (0, 1). \end{cases} \quad (12)$$

- (v) Apply scaling and wavelet functions to extract components of various modes. The approximate coefficients can be represented as the inner product of the analyzed signal  $f$  with the following empirical scaling function:

$$W_f(1, t) = \langle f, \phi_1 \rangle = \int f(\tau) \overline{\phi_1(\tau - t)} d\tau. \quad (13)$$

Similarly, the empirical wavelet with the inner product of analyzed signal  $f$ , are used to define the detailed co-efficient as follows:

$$W_f(i, t) = \langle f, \psi_i \rangle = \int f(\tau) \overline{\psi_i(\tau - t)} d\tau. \quad (14)$$

Here,  $W_f(i, t)$  denotes the detailed coefficients for the  $i$  th filter bank at the  $t^{\text{th}}$  time point.

The steps of implementations of EWT are also shown in Fig. 2.

#### 2.1.3. Kernel principal component analysis

Kernel Principal Component Analysis (KPCA) is an advanced non-dimensionality reduction, classification and feature extraction method used for analyzing nonlinear data, particularly in the context of fault detection and diagnosis. It maps input data into a higher-dimensional feature space using a kernel function, allowing the extraction of principal components in this space. This method effectively captures complex data structures, offering enhanced pattern recognition and feature extraction capabilities. By utilizing kernel functions, KPCA facilitates the computation of dot products in high-dimensional spaces without explicitly performing the high-dimensional mapping, making it efficient for processing and analyzing nonlinear data patterns. Unlike traditional PCA, KPCA does not require pre-specifying the number of principal components or engaging in nonlinear optimization, simplifying its application. KPCA is particularly useful for tasks requiring feature extraction and dimensionality reduction in datasets where linear correlations between variables are insufficient to describe the underlying structure [45–49].

In order to implement KPCA model for structural behavior, first consider  $\{\mathbf{x}_i\}$  is the set of normalized data of structure with  $i = 1, 2, \dots, N$  in a  $D$ -dimensionality space. An  $M$ -dimensional feature space can be created by applying a nonlinear transformation  $\phi$  to each data point  $\mathbf{x}_i$ ,

resulting in a point  $\phi(\mathbf{x}_i)$ . Then a covariance feature matrix which is created with assumption that transformed point in feature space are at center, that is  $\sum_{i=1}^N \phi(\mathbf{x}_i) = 0$ , can be written as [50–52]:

$$\mathbf{C} = \frac{1}{N} \sum_{i=1}^N \phi(\mathbf{x}_i) \phi(\mathbf{x}_i)^T \quad (15)$$

Principal component data are calculated using a formulation based on kernel matrices, where the matrix size corresponds to the data points,  $N$ . Consequently, the eigenvalue problem may be described as follows:

$$Cv_k = \frac{1}{N} \sum_{i=1}^N \phi(\mathbf{x}_i) \{ \phi(\mathbf{x}_i)^T v_k \} = \lambda_k v_k \quad (16)$$

This indicates that  $v_k$  solutions and transformed data points,  $\phi(\mathbf{x}_i)$ , must be in the same space. Consequently, the coefficients  $\alpha_{ki}$  ( $i = 1, \dots, N$ ) exists such that:

$$v_k = \sum_{i=1}^N \alpha_{ki} \phi(\mathbf{x}_i) \quad (17)$$

Therefore, the eigenvalue problem equation can be rewritten as:

$$\frac{1}{N} \sum_{i=1}^N \phi(\mathbf{x}_i) \phi(\mathbf{x}_i)^T \sum_{j=1}^N \alpha_{kj} \phi(\mathbf{x}_i) = \lambda_k \sum_{i=1}^N \alpha_{ki} \phi(\mathbf{x}_i) \quad (18)$$

Now a kernel function is introduced in above equation such that:

$$K_{ij} = \kappa(\mathbf{x}_i, \mathbf{x}_j) = \phi(\mathbf{x}_i) \phi(\mathbf{x}_j) = \phi(\mathbf{x}_i) \cdot \phi(\mathbf{x}_j) \quad (19)$$

We can write the eigenvalue problem like this:

$$\frac{1}{N} \sum_{i=1}^N \kappa(\mathbf{x}_i, \mathbf{x}_i) \sum_{j=1}^N \alpha_{kj} \kappa(\mathbf{x}_i, \mathbf{x}_j) = \lambda_k \sum_{i=1}^N \alpha_{ki} \kappa(\mathbf{x}_i, \mathbf{x}_i) \quad (20)$$

which can be further simplify as:

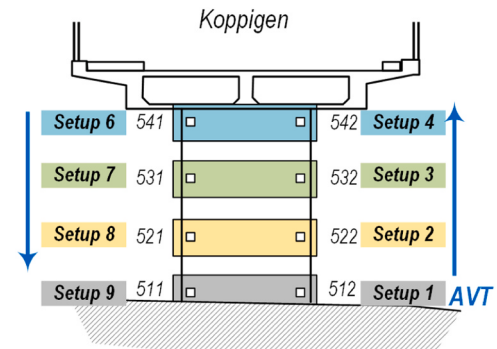


Fig. 5. Accelerometers Location Cross-section view, reproduced from [53].

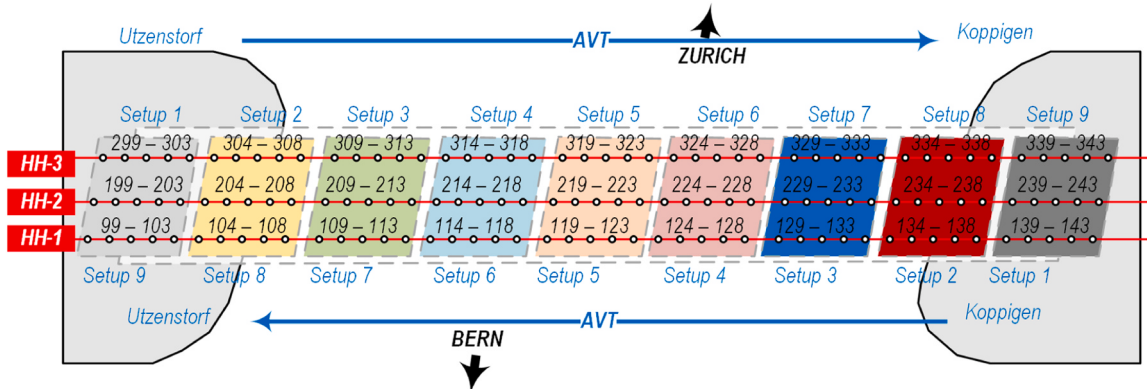


Fig. 4. Accelerometers Location Plan view, reproduced from [53].

**Table 1**

Damage Scenarios for the Z-24 bridge data [53].

Progressive Damage Day	Date (1998)	Damage Scenario
1	4-Aug	Undamaged condition
2	10-Aug	Pier lowered by 20 mm
3	12-Aug	Pier lowered by 40 mm
4	17-Aug	Pier lowered by 80 mm
5	18-Aug	Pier lowered by 95 mm
6	19-Aug	Pier lifted and foundation tilted
7	20-Aug	New reference condition
8	25-Aug	Concrete spalling at soffit, 12 m <sup>2</sup>
9	26-Aug	Concrete spalling at soffit, 24 m <sup>2</sup>
10	27-Aug	Abutment shifted by 1 m
11	31-Aug	Concrete hinge failure
12	2-Sep	Failure of two anchor heads
13	3-Sep	Failure of four anchor heads
14	7-Sep	Rupture of two out of sixteen tendons
15	8-Sep	Rupture of four out of sixteen tendons
16	9-Sep	Rupture of six out of sixteen tendons

$$KK\alpha_i = \lambda_k N K \alpha_k \quad (21)$$

With zero eigenvalues for K, which are irrelevant for the principal components' projection, the aforementioned equation can be redefine as follows:

$$K\alpha_i = \lambda_k N \alpha_k \quad (22)$$

After working out the eigenvalue problem, the N-dimensional column vectors  $\alpha_k$  is employed for x test point principal component for  $k = 1, 2, \dots, M$  using the following formula:

$$y_k(x) = \phi(x)^T v_k = \sum_{i=1}^N \alpha_i \kappa(x, x_k) \quad (23)$$

Initially, data set {f(xi)} was considered to have zero mean, but it might not represent true state. So the Gram matrix can be substituted with kernel matrix K as shown below:

$$\bar{K} = K - \mathbf{1}_N K - K \mathbf{1}_N + \mathbf{1}_N K \mathbf{1}_N \quad (24)$$

where  $\mathbf{1}_N$  is an  $N \times N$  matrix with all elements  $1/N$ .

Besides feature extraction, KPCA can also detect anomalies. In normal conditions, the projected data of main and residual space should be within a specific region and any deviation from that region show the anomalies in system. Hotelling's  $T^2$  and Squared Prediction Error (SPE) are two parameters often used to describe the projection size in the main and residual space. Hotelling's  $T^2$  is a statistical tool commonly used in

**Table 2**

metrics parameter for performance.

Sr.	Metrics Parameters	Proposed Methodology	EMD + KPCA	EWT + KPCA
1	Accuracy	1.00	0.9141	0.9531
2	Precision	1.00	0.4	0.5714
3	Sensitivity	1.00	0.75	0.95
4	F <sub>1</sub> Score	1.00	0.5217	0.7273

**Table 3**  
Timeline of Testing of RC bridge.

Day	Date
1	01/01/2024
2	04/02/2024
3	05/02/2024
4	06/02/2024
5	08/02/2024
6	10/02/2024
7	13/02/2024
8	15/02/2024
9	16/02/2024

quality control and process monitoring to identify deviations from a target performance. Essentially, it's an extension of the Student's *t*-test into multiple dimensions. Variation of the test vector in the main space may be measured using Hotelling's  $T^2$  tool. It calculates the distance from the test vector to the center point of the sample mean. This method uses the sample mean, covariance, and size to calculate the  $T^2$  statistic, which is then compared to a critical value from Hotelling's distribution to check for a significant difference between the observed mean and the theoretical mean. The expression of Hotelling's  $T^2$  is as follows:

$$T^2 = \mathbf{x} \mathbf{P} \Lambda^{-1} \mathbf{P}^T \mathbf{x}^T \leq T_a^2 \text{ where, } T_a^2 = \delta_a^2 = \frac{k(n-1)(n+1)}{n(n-k)} F_\alpha(k, n-k) \quad (25)$$

The load matrix is represented by P and the diagonal matrix is implied as  $\Lambda$  with the eigenvalues in declining order and the first k eigenvalues is used in the covariance matrix.  $T_a^2$  mark the boundaries of Hotelling's  $T^2$ , with F is one of the distributions, n represents the number of principal components and  $F_\alpha(k, n-k)$  is the benchmark at confidence level 1- $\alpha$ .

The SPE, also referred to as Q-statistics, serves as a metric to gauge the dissimilarity between observed and predicted values within a model. Its primary purpose is to pinpoint outliers or anomalies in a dataset that the model struggles to explain effectively. In the realm of process monitoring, a heightened SPE value signals a notable departure from the usual process behavior, hinting at possible issues or alterations in the process. To compute SPE, the square of the difference between actual data points and their corresponding values predicted by the model is calculated. Elevated SPE values point towards substantial deviations, potentially indicating process faults or outliers. It can be mathematically express as:

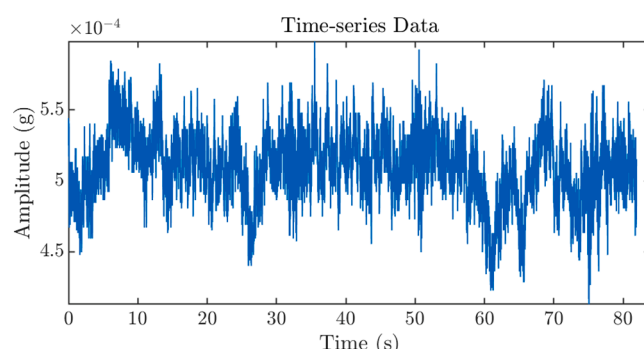
$$Q = \|e\|^2 = \|x - \hat{x}\|^2 = \|x - x \mathbf{P} \mathbf{P}^T\|^2 \leq Q_a \text{ where, } Q_a = \xi \chi_{h,a}^2 \quad (26)$$

Where,  $\xi$  can be computed as  $\gamma_2/\gamma_1$ ,  $h$  can be computed using integer  $(\gamma_1^2 - \gamma_2)$ , integer (0) is representing the integer value of  $o$  and  $\chi_{h,a}$  is actually  $h$  degrees freedom Chi-square distribution. The constant  $\gamma_c$  can be computed as  $\gamma_c = \sum_{k=l+1}^m \lambda_k^c$  with  $\lambda_k^c$  represent the  $k^{\text{th}}$  eigenvalue to the  $c^{\text{th}}$  power ( $c = \{1, 2\}$ ) [49].

## 2.2. Proposed damage detection methodology

In this section, a detailed methodology to implement the combination of CEEMDAN, EWT and KPCA for feature extraction and damage detection is explained. Following is the procedure step to detect damage in the structure:

- The first step in the pipeline of damage detection is the collection of numerical or experimental vibrations data of the bridge for real time health monitoring. An ambient vibration test is performed

**Fig. 6.** Original Signals of 238 V accelerometer.

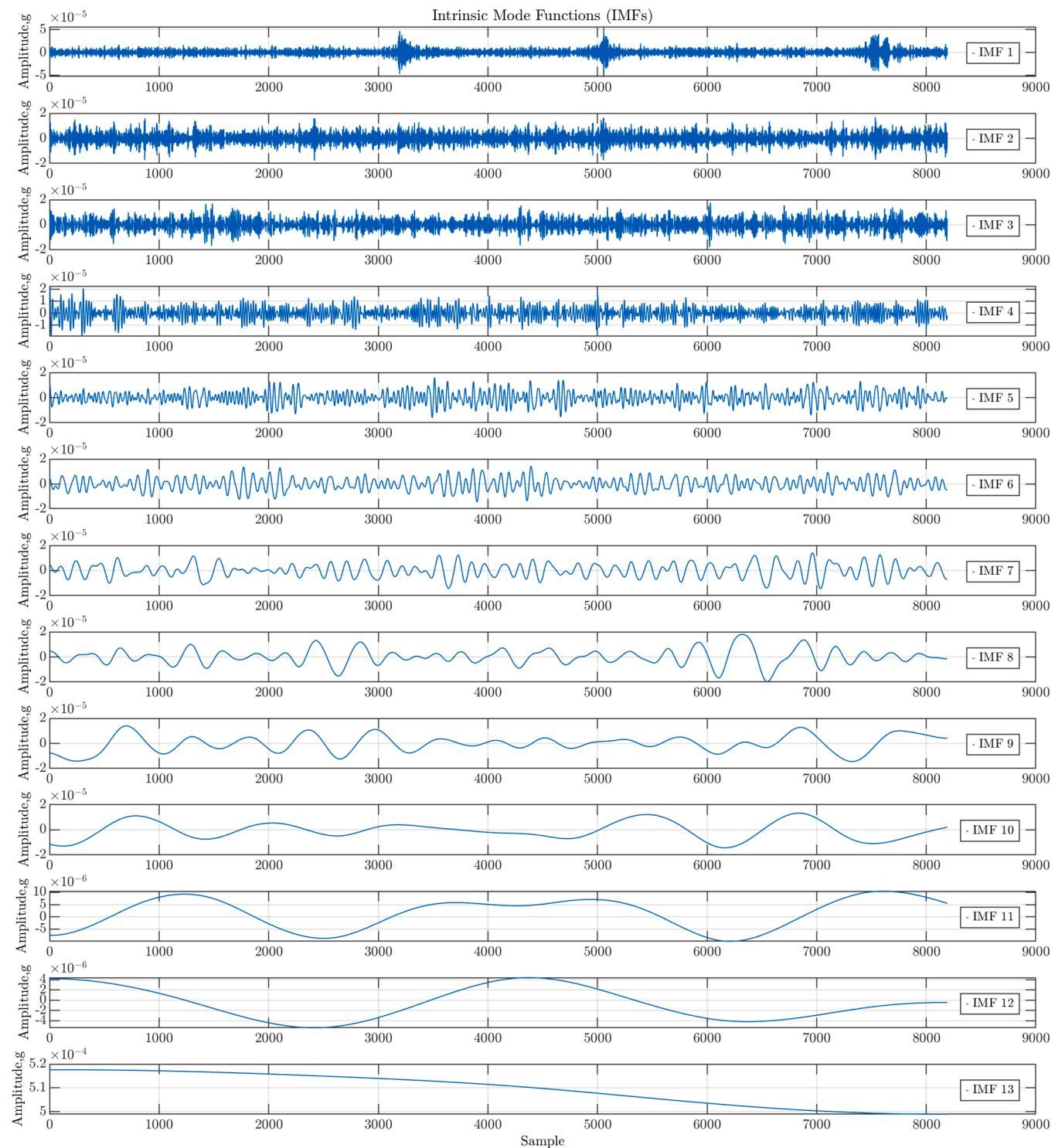


**Fig. 7.** Results of CEEMDAN for un-damaged state of 238 V accelerometer.

- on the bridge in healthy state without any damage and accelerometers are used to capture these vibrations data.
- (ii) These vibrations data are then subject to feature extraction process of CEEMDAN, in which with the help of adaptive noise and empirical mode decomposition, IMFs are obtained. These IMFs are the oscillatory components having distinct frequencies and amplitudes.

(iii) Now a correlation coefficient ( $r_{ci}$ ) is calculated between each IMFs and original signals using the following expression:

$$r_{ci} = \left| \frac{\sum_{t=1}^n (x(t) - \bar{x})(c_i(t) - \bar{c}_i)}{\sigma_{c_i} \sigma_x} \right| \quad (27)$$

where,  $x(t)$  is the original signals,  $c_i(t)$  is the  $i^{\text{th}}$  IMF decomposed

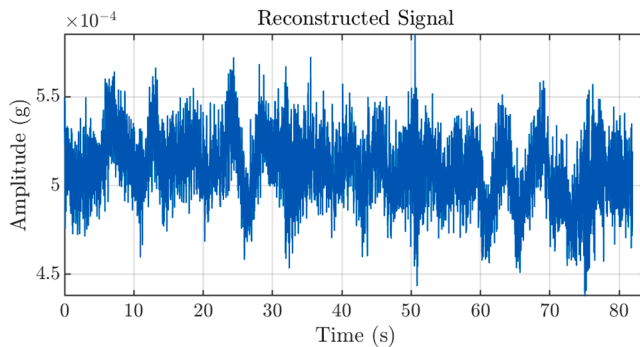


**Fig. 8.** Reconstructed Signals of undamaged state for 238 V accelerometer.

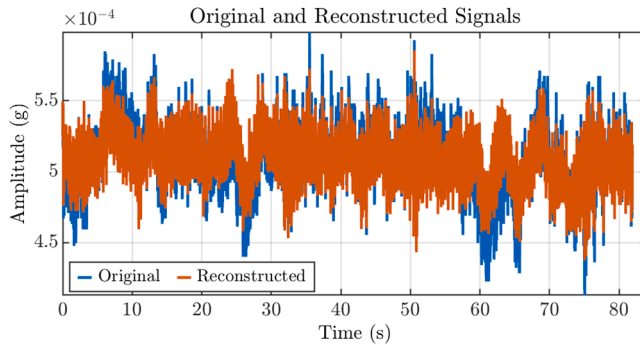


**Fig. 9.** Comparison of Original and Reconstructed Signals of undamaged state for 238 V accelerometer.

using CEEMDAN;  $\sigma_{c_i}$  and  $\sigma_x$  are refer as standard deviations of  $c_i$  and  $x(t)$ ; and  $\bar{c}_i$  and  $\bar{x}$  represent the mean values of IMFs  $c_i$  and original signals  $x(t)$ , respectively.

(iv) Also, calculate the kurtosis  $k_{c_i}$  of each IMFs, which represent the flatness of peaks, using following expression:

$$k_{c_i} = \frac{\sum (c_i(t) - \bar{c}_i)^4}{(N-1)\sigma_{c_i}^4} \quad (28)$$

where,  $c_i(t)$  is the  $i^{\text{th}}$  IMF decomposed using CEEMDAN;  $\sigma_{c_i}$  are refer as standard deviations of  $c_i$ ;  $\bar{c}_i$  represent the mean values of IMFs  $c_i$ ; and  $N$  is refer as the length of signal  $c_i(t)$ .

(v) After calculating the above two parameters a sensitive IMF evaluation index (SIEI) is created, which can be represented as:

$$I_{SIEI}(i) = \frac{r_{c_i}}{\sum r_{c_i}} + \frac{k_{c_i}}{\sum k_{c_i}}. \quad (29)$$

(vi) Arrange these SIEI values in descending order, in which the highest values of SIEI represent the important features and lowest values represent noise. So, IMF of large SIEI values is selected as an effective IMFs ( $K'$ ), for reconstruction of signals which represent the clear or denoising signal  $x_{\text{clear}}(t)$  as:

$$x_{\text{clear}}(t) = \sum_{k=1}^{K'} c_k(t) \quad (30)$$

(vii) Feature extraction is subsequently conducted on the reconstructed signals in the time domain to generate feature vectors.

This conversion involves utilizing Empirical Wavelet Transform (EWT) to translate the data into the time-frequency domain. The clear signals without noise are analyzed by EWT, which help to decompose reconstructed signals into a set of elementary signals called empirical wavelets, which are localized in both time and frequency. This step allows for a detailed spectral analysis of the reconstructed signals, enhancing the identification of intrinsic modes linked to different physical phenomena. This combination can address CEEMDAN's limitations by providing a clearer distinction between modes that may be closely spaced in frequency, as the reconstructed signals are decomposed again to improve the accuracy of feature extraction. The result is a more refined analysis of the acceleration data, potentially leading to better damage detection in structures by isolating and analyzing specific frequency bands associated with damage indicators.

(viii) Spectral centroid (SC) serves as the chosen damage sensitive feature for extraction from isolated modes of EWT process, by utilizing STFT analysis. This parameter, intricately linked to the spectrum's shape, signifies the center of gravity within each block's spectrum and helps in damage detection process. The determination of spectral centroid for each EWT decomposition involves computing the weighted average of frequencies present in the signal. The weights are assigned based on the spectrum's magnitude at each frequency, thereby spotlighting the predominant frequency within each decomposed mode of EWT. Mathematically, it is expressed as follows:

$$SC_i = \frac{\sum_0^{k/2-1} k \cdot |X(k,j)|^2}{\sum_0^{k/2-1} |X(k,j)|^2} \quad (31)$$

Here,  $X(k,j)$  represents the STFT analysis magnitude spectrum, with  $k$  and  $j$  denoting the block size and block index, respectively and  $SC_i$  represents the spectral centroids of individual decomposed  $i^{\text{th}}$  IMF.

(ix) To detect structural damage, the feature matrix  $SC_i$  is projected onto a KPCA model with a Gaussian kernel. There are two steps to this process: training and monitoring. During the training phase, data is collected under baseline settings, indicating the structure's expected healthy state. This dataset is critical to constructing the model and determining control limits. In this phase, KPCA is utilized to compute kernel principal components, resulting in a reduced-dimensional representation of the initial data.

(x) This crucial phase creates new and uncorrelated characteristics that are arranged by variance from the feature matrix. It helps detect damage from noise or environmental factors by differentiating features with significant deviations from healthy state. This reduction makes it possible to create a model of the intact structure, which is subsequently used in the monitoring phase to diagnose structural health conditions.

(xi) A new dataset consisting of measured parameters (the feature matrix of spectral centroids) is prepared in the monitoring phase, to maintain consistency with the samples used during the training phase. The projections are then obtained by projecting this dataset into the KPCA model. The  $T^2$  and SPE, critical indicators of damage sensitivity, are computed and evaluated against baseline values. Detection of damage relies on monitoring inconsistencies in  $T^2$  and SPE chart readings. When these indices surpass predetermined criteria establish during the baseline phase, damage is detected.

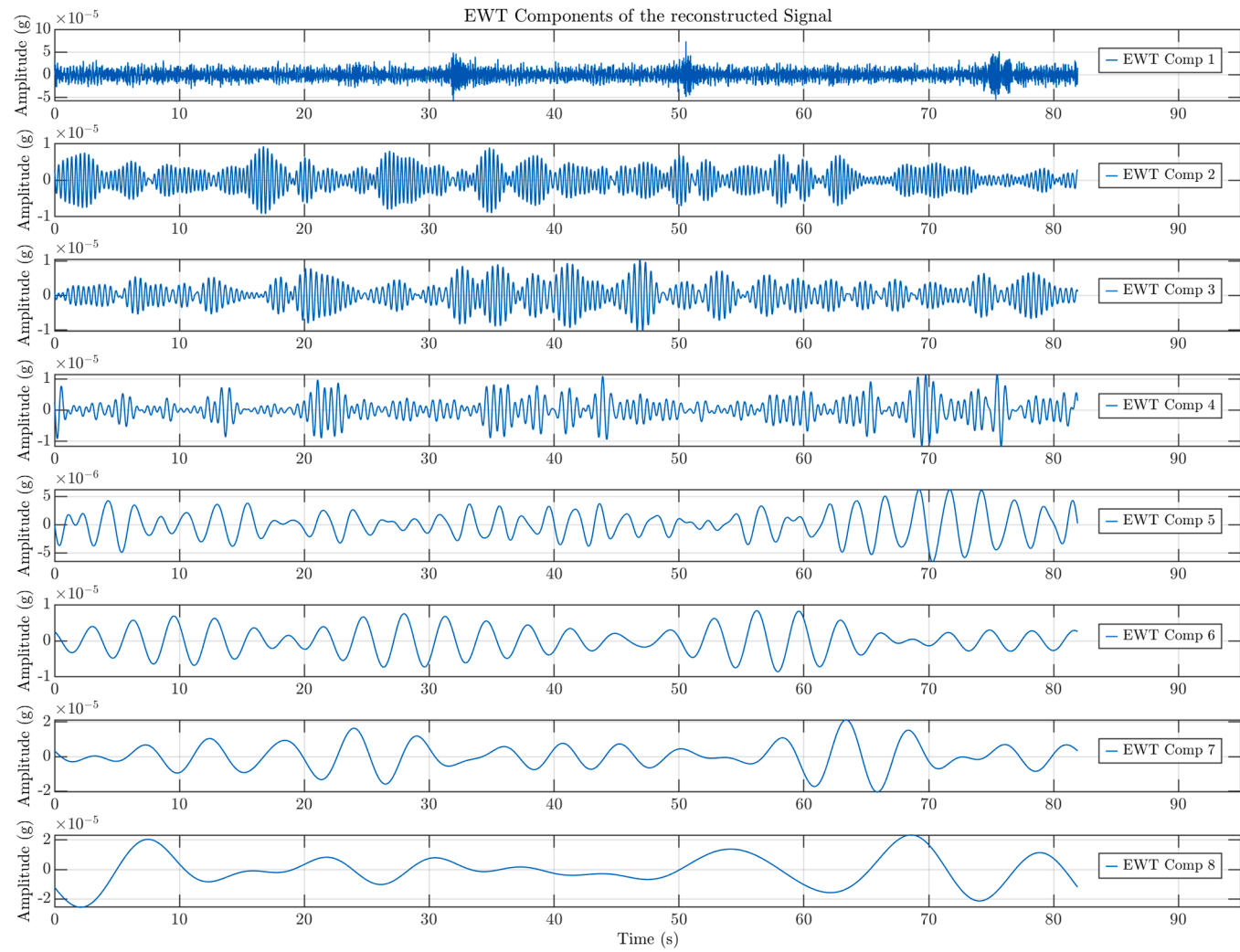


**Fig. 10.** EWT IMF for un-damage state of reconstructed signals of 238 V accelerometer.

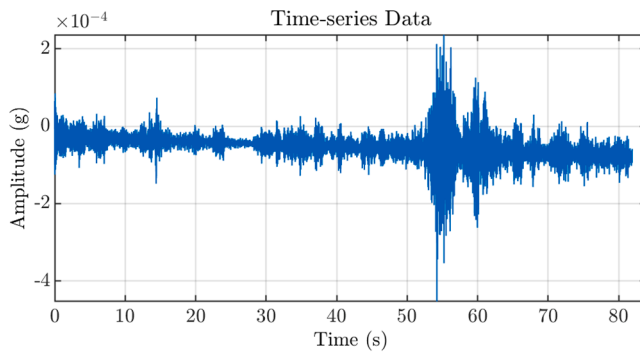


**Fig. 11.** Original Signals of 238 V accelerometer on 10 Aug 1998.

### 3. Application of proposed methodology

#### 3.1. Z-24 bridge

This damage detection method was validated using benchmark data from the Z-24 bridge. The Z-24 bridge, which over the A1 motorway that connected Bern and Zürich, was a vital connection between Koppigen

and Utzenstorf in the Bern canton, Switzerland. This bridge was a traditional post-tensioned concrete two-cell box girder, measuring 58 m in length overall with a 30-meter main span and two 14-meter side spans, as shown in Fig. 3. At the end of 1998, the bridge was finally dismantled after a series of progressive damage tests and extensive long-term monitoring.

Before it was demolished, the bridge underwent several tests, including PDT and a long-term continuous monitoring test conducted the year prior, with main aim was measuring the environmental variance in the dynamics of the bridge. A month-long series of progressive damage testing preceded the destruction was arranged to demonstrate real-world deterioration influence in bridge dynamics.

The database of accelerometric measurements, which is accessible for research, was established as part of the "System Identification to Monitor Civil Engineering Structures" (SIMCES) European Brite EuRam research project BE-3157. All data are available on the SIMCES project website [53].

##### 3.1.1. Data collection

The project used force-balance-type FBA-11 accelerometers by Kinematics, which had high sensitivity, reliability, and low power consumption. The accelerometers were of 16-bit resolution and had 100 Hz sampling rate. The locations and measurement axes of the accelerometers are shown in Fig. 4 and Fig. 5. Each sensor collected 65,536 samples every hour at a sampling rate of 100 Hz, resulting in an

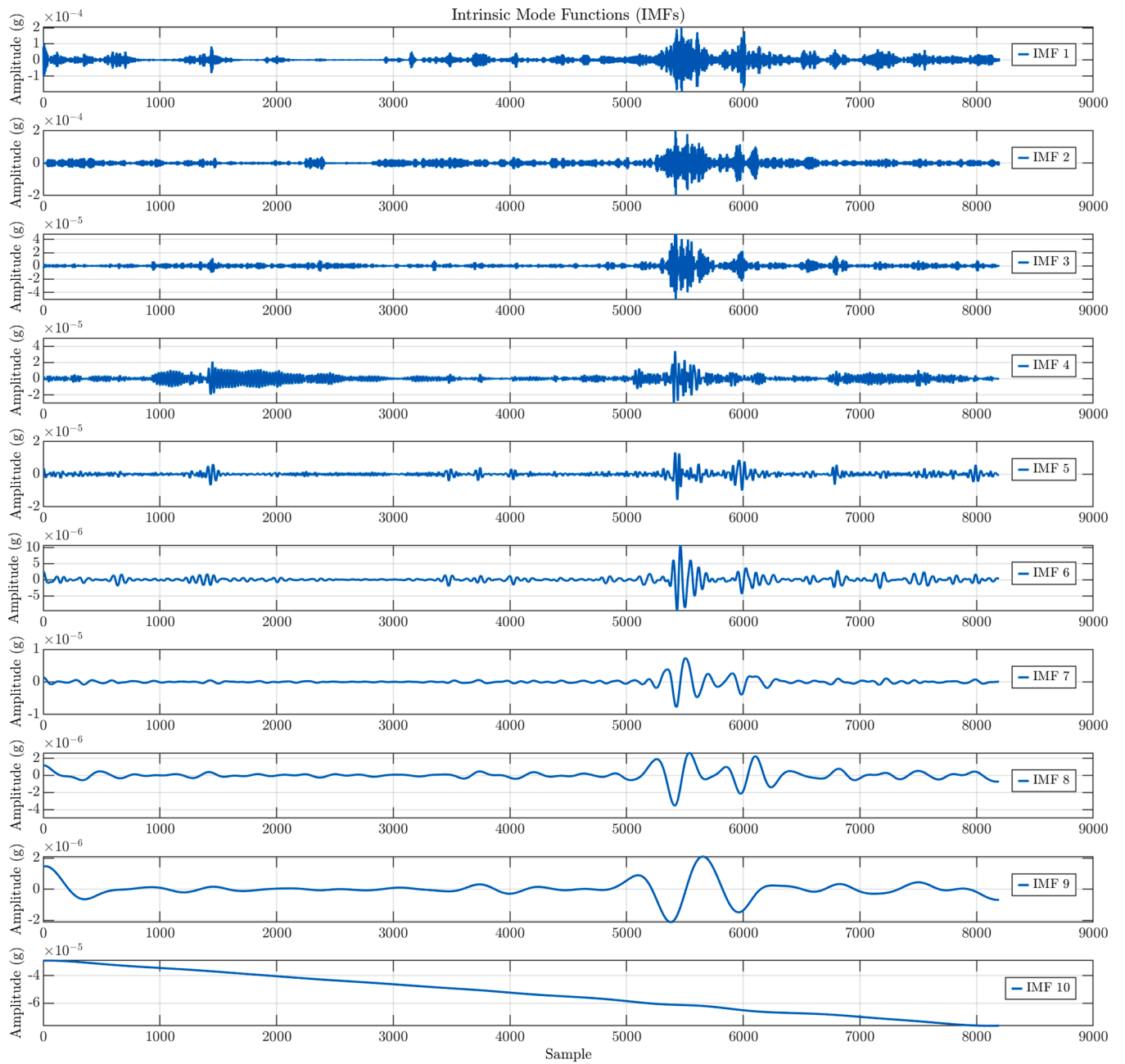


**Fig. 12.** Results of CEEMDAN for Damage state (10 Aug) for 238 V accelerometer.

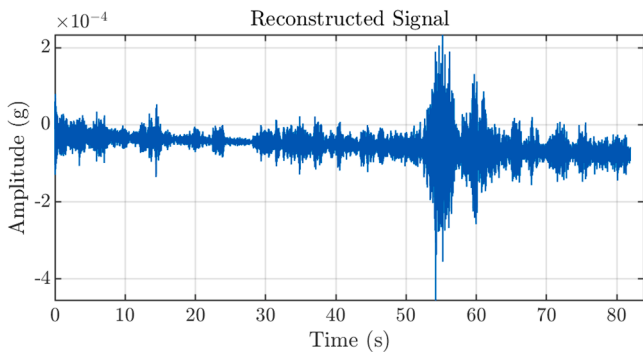


**Fig. 13.** Reconstructed Signals of 238 V at 10 Aug 1998.

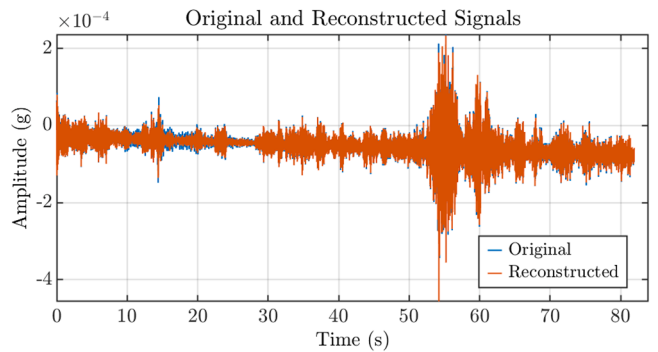


**Fig. 14.** Comparison of Original and Reconstructed Signals of 238 V accelerometer at 10 Aug 1998.

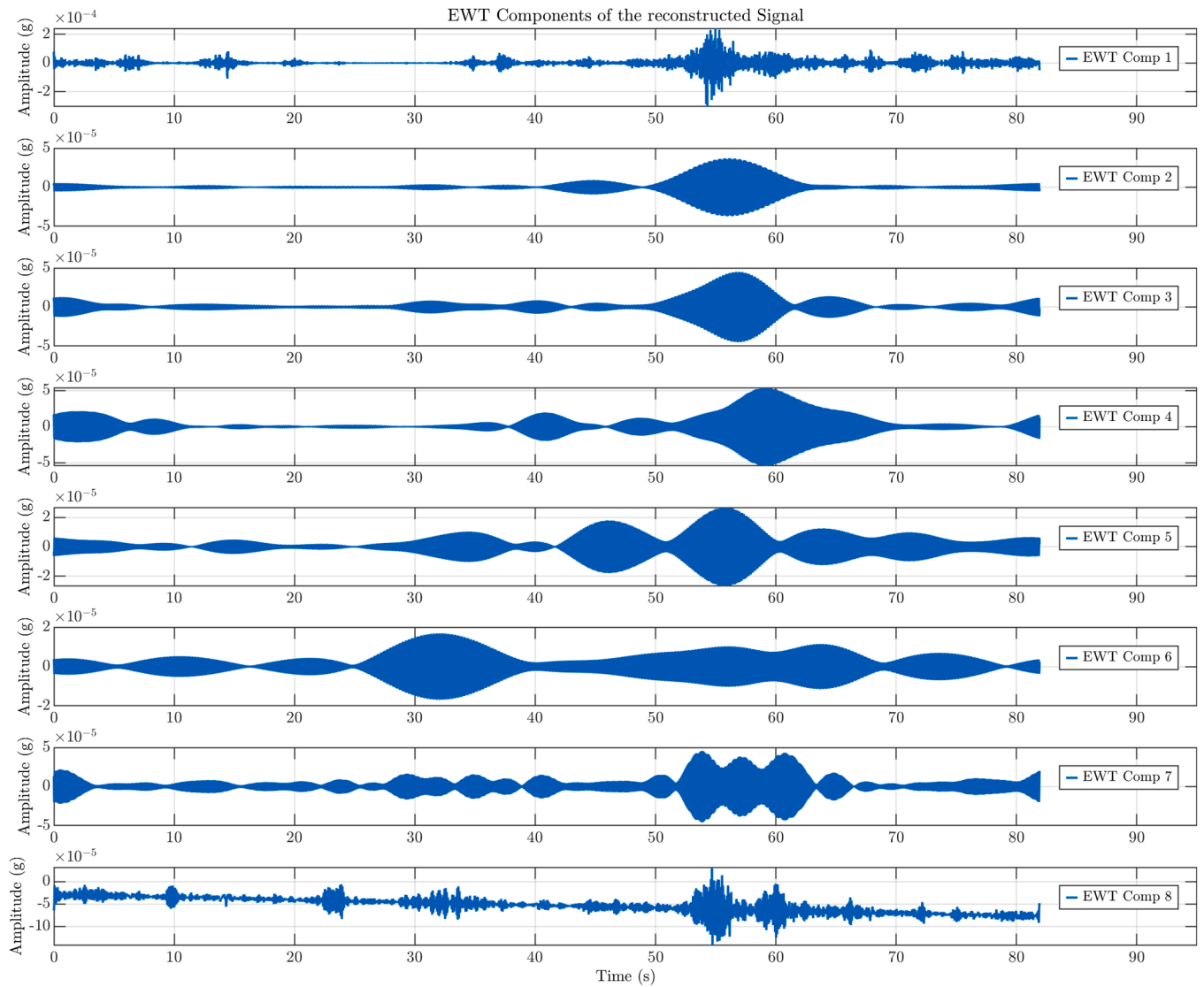


Fig. 15. EWT of reconstructed signals for damage state of 10 Aug 1998.

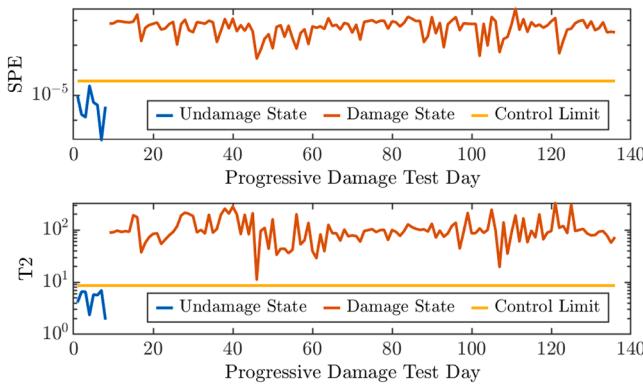


Fig. 16. Damage detection in 238 V accelerometer using KPCA.

acquisition period of 655.36 seconds. For this study, two accelerometers including 238 V and 243 V were selected to access the vertical accelerations data.

### 3.1.2. Progressive damage test

In order to detect damage, progressive damage tests were conducted

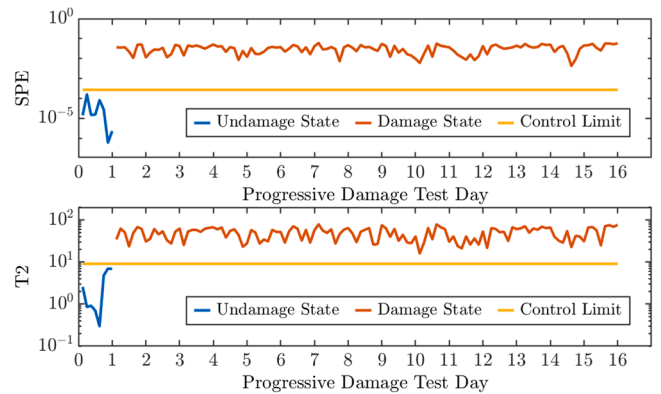


Fig. 17. Damage detection in 243 V accelerometer using KPCA.

over the course of a month before the bridge's full demolition. These evaluations were crucial for ensuring the bridge's safety, focusing on damage types that are commonly encountered. Table 1 provides a detailed summary of these tests. The measurements encompassed 291 degrees of freedom, capturing movements of the pillars and primarily

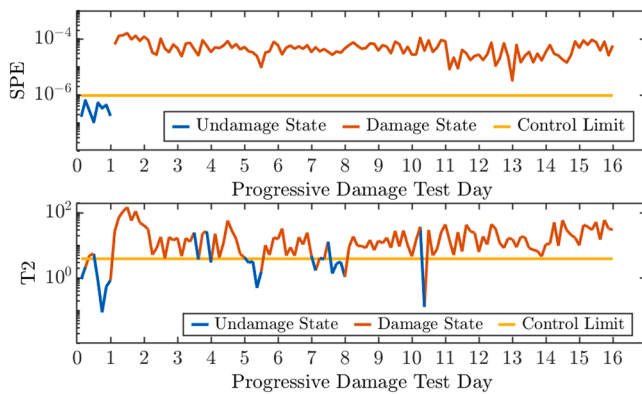


Fig. 18. Damage Detection results of EMD-KPCA for accelerometer 238 V.

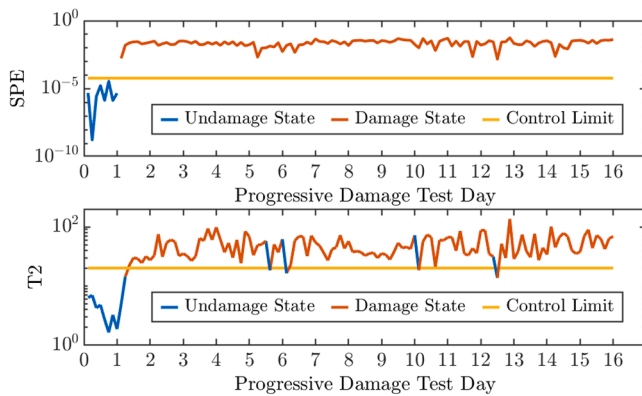


Fig. 19. Damage Detection results of EWT-KPCA for accelerometer 238 V.

		Actual Values	
		Positive	Negative
Predicted Values	Positive	8	0
	Negative	0	120

Fig. 20. Confusion Matrix of Proposed Methodology.

detecting vertical and lateral shifts on the bridge deck.

### 3.1.3. Damage detection

First, the raw acceleration data of 238 V accelerometer obtained from ambient vibration test were taken. And these vibrations data were subjected to CEEMDAN. Then, with the help of adaptive noise and empirical mode decomposition, IMFs were obtained. Each IMF helps to distinguish the frequency content in the vibrations data into distinct model, which were then analyzed and SIEI was calculated. Then, after hit and trail method, a value of 0.15 was taken as minimum value of SIEI of IMFs, to distinguish noise and environmental variations from the signals. Therefore, the IMFs having value greater than 0.15 were added to reconstruct the signals. Then EWT was utilized, which helped to decompose reconstructed signals into multiresolution analysis (MRA) components for a detailed spectral analysis of the reconstructed signals,

		Actual Values	
		Positive	Negative
Predicted Values	Positive	6	9
	Negative	2	111

Fig. 21. Confusion Matrix of EMD-KPCA.

		Actual Values	
		Positive	Negative
Predicted Values	Positive	8	6
	Negative	0	114

Fig. 22. Confusion Matrix of EWT-KPCA.

enhancing the identification of intrinsic modes linked to different physical phenomena. For illustration, a few results of CEEMDAN and EWT for both un-damage and damage state are shown in Figs. 6–15.

After obtaining the multiresolution analysis (MRA) components the spectral centroids (SC) were extracted as a damage sensitive feature. The determination of spectral centroid for each EWT decomposition involved computing the weighted average of frequencies present in the signal. For damage detection in the structure the feature matrix  $SC_i$  underwent projection into the kernel PCA model utilizing a Gaussian kernel. This step consisted of two phases: training phase and monitoring phase. In the training phase, baseline data, which was collected on day 1 was utilized, representing a presumed healthy state of the structure. This dataset was pivotal for model construction and the establishment of control limits. The damage data that was collected after day one was then used during the monitoring phase. Following that, the dataset was projected into the KPCA model, resulting in the calculation and comparison of the  $T^2$ -statistic and Q-statistic (SPE) with baseline values. As damage detection depends on tracking changes in the SPE and  $T^2$  chart values, therefore, when damage index values exceeded the threshold calculated in the baseline phase, damage was detected. It can be clearly seen from the results that the damage state and the healthy condition are distinctly separated from one another. Damage detection results of 238 V accelerometers are shown in Fig. 16.

The same procedure was repeated on 243 V accelerometer for damage detection. KPCA model was employed with variance of 95 % and gamma value of 128, these values were chosen through hit and trail method to get the best results. A variance threshold was chosen based on the principle of capturing the most significant structural features. This threshold ensured that the principal components with the largest eigenvalues, which represented the dominant variability in the data, were retained, while those dominated by noise or redundancy were excluded.

To effectively implement the dimensionality reduction step in KPCA,

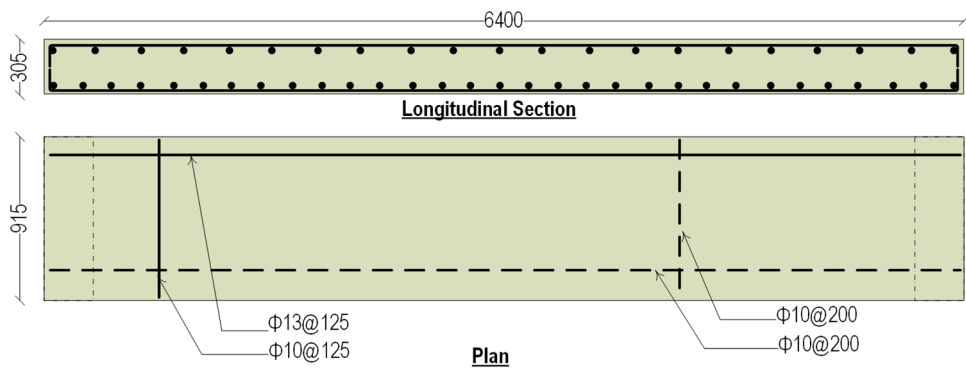


Fig. 23. Reinforcement Detailing of RC bridge slab (mm units).

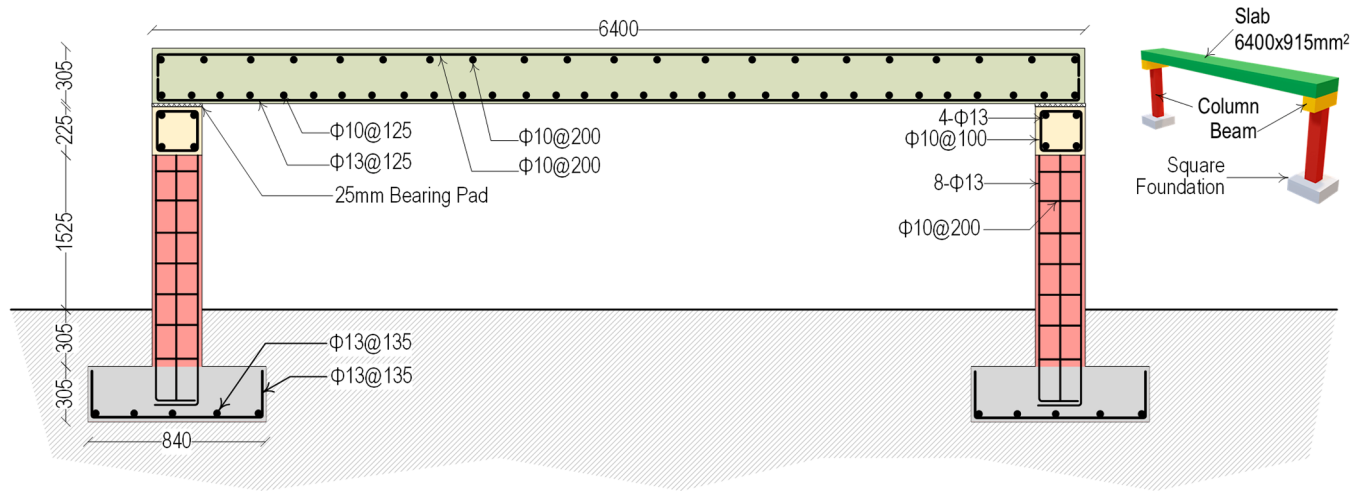


Fig. 24. RC Bridge structural elements and reinforcement details (mm unit).

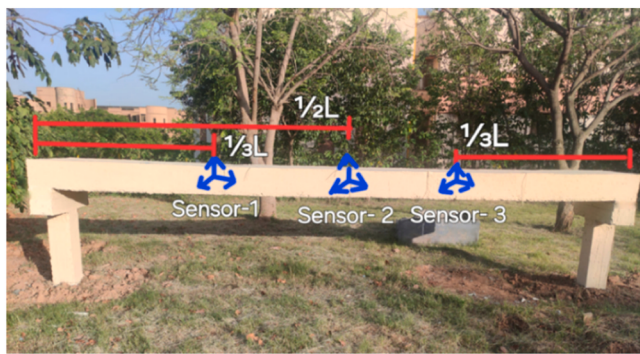


Fig. 25. RC Bridge constructed in NUST with sensors locations.

the eigenvalue spectrum of the spectral centroid feature matrix was computed during the baseline phase. This feature matrix, derived from spectral centroids after preprocessing with CEEMDAN and EWT, was subjected to eigenvalue decomposition. The eigenvalues were sorted in descending order to facilitate cumulative variance analysis, enabling the identification of the optimal threshold for retaining principal components. A 95 % cumulative variance threshold was selected, as it ensured the inclusion of all significant structural features (represented by principal components with high eigenvalues) while excluding components dominated by noise or redundancy, which typically correspond to low eigenvalues.

While the tuning of the  $\gamma$  parameter in KPCA was performed to

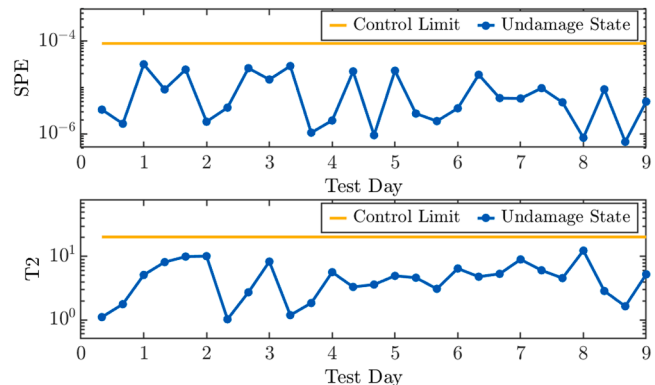
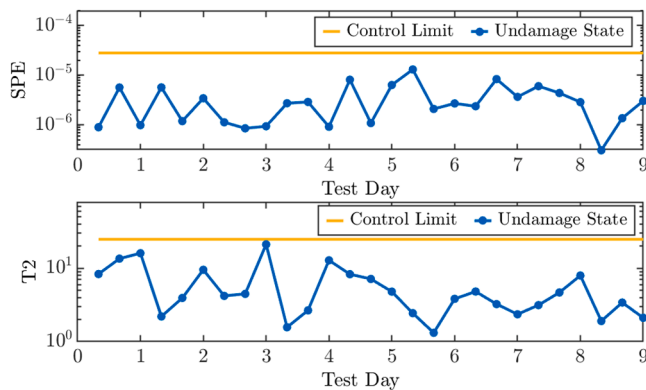
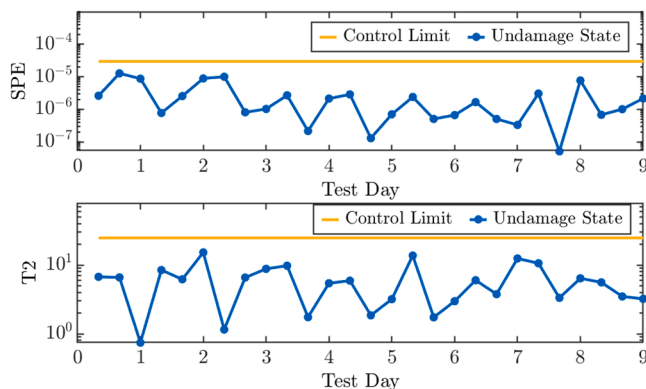


Fig. 26. Health monitoring results of accelerometer placed on RC bridge at 1/3rd location from right.

optimize the Gaussian kernel's ability to separate data points corresponding to healthy states and hypothetical damage scenarios within the trans-formed feature space. This process began by calculating pairwise distances within the baseline feature matrix (healthy state data) to understand the data's spatial relationships in the original high-dimensional space. For each  $\gamma$  value, the Gaussian kernel matrix was constructed, transforming the data into a space where damage-sensitive indicators ( $T^2$  and SPE) could be evaluated. Gamma was iteratively adjusted by testing different ranges of values to identify the parameter that maximized the separation between healthy and damaged states. The selection



**Fig. 27.** Health monitoring results of accelerometer placed on RC bridge at 1/2 location from right.



**Fig. 28.** Health monitoring results of accelerometer placed on RC bridge at 1/3rd location from left.

criteria included sensitivity to minor damage, ensuring subtle changes in structural behavior were detectable, and robustness against noise and environmental variability, minimizing false alarms. Ultimately,  $\gamma = 128$  was selected as the optimal balance, resulting in clear clustering of healthy and damaged states in the KPCA-transformed space and enhancing the performance of  $T^2$  and SPE damage indicators. This systematic approach ensured that the KPCA model effectively captured structural variability while remaining robust in practical applications [54–56]. The damage detection results are shown in Fig. 17.

#### 3.1.4. F1-score

In order to check the efficiency and applicability of the proposed methodology, f1-score test was calculated for 238 V accelerometer and results were compared with two most commonly used methods EMD-KPCA [8,13–15] and EWT-KPCA [57]. So, in case of EMD-KPCA the accelerations data of all days were first processed through EMD and then put into KPCA algorithm for damage detection. Similarly, in case of EWT-KPCA, vibration data was processed by EWT followed by KPCA for damage detection. The results of both these cases are shown in Figs. 18 and 19, respectively.:.

Then following metrics were used to check the performance of proposed methodology:

$$\text{Accuracy} = \frac{T_p + T_N}{T_p + T_N + F_p + F_N} \quad (32)$$

$$\text{Precision} = \frac{T_p}{T_p + F_p} \quad (33)$$

$$\text{Sensitivity} = \frac{T_p}{T_p + F_N} \quad (34)$$

$$F_1\text{score} = 2 \cdot \frac{\text{Sensitivity} \cdot \text{Precision}}{\text{Sensitivity} + \text{Precision}} \quad (35)$$

where  $T_p$ ,  $T_N$ ,  $F_p$ , and  $F_N$  represent, respectively, true positive, true negative, false positive, and false negative predictions. To calculate the following parameter, a confusion matrix was constructed, as shown in Figs. 20–22.

The evaluated metrics parameter for performance evaluation are as follows:

These performance metrics clearly shows that, the proposed methodology clearly effective in distinguishing noise and environmental factors from the vibrations data, making the results more effective with accuracy of 100 %.

### 3.2. Prototype reinforced concrete (RC) bridge

To evaluate the applicability of the proposed damage detection methodology, an RC bridge was constructed in National University of Science and Technology (NUST), Islamabad, Pakistan. The bridge was designed by utilizing the provisions of AASTHO [58] and ACI 318–19 [59], aiming to monitor it in real-time and being used as a testbed for sensor development. The bridge spanning 21 feet was constructed with concrete strength of 3000 psi and steel reinforcement yielding limit of 60,000 psi. The detail of reinforcement and bridge are shown in Fig. 23 and Fig. 24 respectively.

#### 3.2.1. Ambient vibration test

To accommodate real-time health monitoring of this RC bridge, a G-Link-200 accelerometer was used. The accelerometers were placed as represented in Fig. 25. The sampling frequency of each accelerometer was set to 4096 Hz. To introduce impact vibrations, an impact hammer was used to create the vibration at 6 locations, which were at equal distance (3' c/c). After testing, the acquired acceleration data was transferred using Sensor Connect software, then the proposed methodology was performed on extracted data of each accelerometer. First the raw accelerations data was processed using CEEMDAN, where the extracted signals were divided into IMFs. Then SIEI was calculated for each signal and after several hit-and-trails, 0.15 value of SIEI was set as the limit of IMFs. The IMFs value greater than 0.15 were then added to reconstruct the signal without noise. These reconstructed signals were then processed using EWT, where signals were converted into mono-components. To access the current condition of bridge, spectral centroids are then calculated as a damage sensitive feature.

The real-time monitoring of bridge was done for 9 days, where day 1 was used as a baseline as no damage were introduced initially in the bridge. The timeline of testing is given as follows:

KPCA model was trained by using the day 1 data as baseline data, as no damage was introduced. And then to access the current condition of bridge, rest of the 8 days data was processed through the KPCA model. The procedure was repeated for all 3 accelerometers, the results of which are shown in Figs. 26–28:

From the above results, it is evident that no damage was detected, which was true as no external damaged was introduced in the bridge throughout the span of time.

### 4. Conclusion

In this study, an advanced methodology employing CEEMDAN and EWT is introduced for enhanced damage detection in bridge structures amidst environmental and operational variations. The spectral centroids feature matrix, derived from the decomposed modes, is efficiently condensed and projected using KPCA to mitigate the effects of

environmental factors. The robustness and applicability of this method are confirmed through empirical validation using data from the Z-24 bridge. The experimental findings and a thorough examination of the IMFs show how well the approach distinguishes between the bridge's healthy and damaged states. This method is noteworthy for its ability to isolate the SC features from specific IMFs, significantly enhancing the feature extraction process by eliminating noise and other information that could impede the identification of structural damage. The ability of the suggested damage indices to effectively detect damage in a variety of scenarios, such as progressive damage tests on the Z-24 Bridge and RC bridge, demonstrates the approach's efficacy and highlights its potential to precisely identify damage even in presence of operational and environmental challenges. Moreover, the calculation of metric performance parameters also indicates that the proposed methodology classifies the damage and undamaged state with accuracy and precision of 100 %. And the proposed methodology on the RC bridge, indicate that no damage introduced in the bridge, which was the actual scenario. This makes the proposed methodology fully applicable for real-time health monitoring. This research also overcomes the issue of the traditional signal decomposition method that struggles in distinguishing the frequency content when there is significant overlap between the frequencies, by removing the irrelevant frequency content while preserving the damage sensitive features. This research marks a significant advancement in the field of structural health monitoring by providing a robust, reliable, and scalable solution that can be applied to various types of bridge structures, ensuring their safety and integrity in the face of diverse and challenging operational environments. For future studies, the damage quantification into the methodology could further enhance its ability to assess the severity of damage and provide more detailed insights for structural health monitoring.

#### CRediT authorship contribution statement

**Hassan Muhammad Usman:** Writing – review & editing, Validation, Project administration, Methodology, Investigation. **Hanif Muhammad Usman:** Writing – review & editing, Supervision, Conceptualization. **Abdullah Hamza Ahsan:** Writing – original draft, Visualization, Software, Formal analysis, Conceptualization. **Ali Ather:** Supervision, Software, Resources, Project administration, Funding acquisition. **Khan Shaukat Ali:** Visualization, Validation, Supervision, Conceptualization. **Shahid Janita Mahnoor:** Validation, Software, Resources, Methodology, Investigation, Formal analysis.

#### Declaration of Competing Interest

The authors declare that they have no known competing financial interests or personal relationships that could have appeared to influence the work reported in this paper.

#### Acknowledgement

This research was supported by the Research and Development Division of Higher Education Commission, Pakistan (No. 20-16068/NRPU/R&D/HEC/2021, 2021).

#### Data Availability

Data will be made available on request.

#### References

- [1] Schulz A, Zia A, Koliba C. Adapting bridge infrastructure to climate change: institutionalizing resilience in intergovernmental transportation planning processes in the Northeastern USA. *Mitig Adapt Strateg Glob Chang* Jan. 2017;22(1):175–98. <https://doi.org/10.1007/s11027-015-9672-x>.
- [2] J.R. Casas and J.J. Moughty, Bridge damage detection based on vibration data: Past and new developments, Feb. 03, 2017, *Frontiers Media S.A.* doi: 10.3389/fbuil.2017.00004.
- [3] Martin Andrew J. Concrete bridges in sustainable development. *Eng Sustain* 157 2004;(4):219–30.
- [4] Kashif Ur Rehman S, Ibrahim Z, Memon SA, Jameel M. Nondestructive Test Methods For Concrete Bridges: A review. Elsevier Ltd; Mar. 15, 2016. <https://doi.org/10.1016/j.conbuildmat.2015.12.011>.
- [5] Ranyal E, Sadhu A, Jain K. Road Condition Monitoring Using Smart Sensing and Artificial Intelligence: A Review. MDPI; Apr. 01, 2022. <https://doi.org/10.3390/s22083044>.
- [6] Farrar CR, Worden K. An introduction to structural health monitoring. *Philos Trans R Soc A: Math, Phys Eng Sci* Feb. 2007;365(1851):303–15. <https://doi.org/10.1098/rsta.2006.1928>.
- [7] Sun L, Shang Z, Xia Y, Bhowmick S, Nagarajaiah S. Review of bridge structural health monitoring aided by big data and artificial intelligence: from condition assessment to damage detection. *J Struct Eng May* 2020;146(5). [https://doi.org/10.1061/\(asce\)st.1943-541x.0002535](https://doi.org/10.1061/(asce)st.1943-541x.0002535).
- [8] Bisheli HB, Amiri GG. Structural damage detection based on variational mode decomposition and kernel PCA-based support vector machine. *Eng Struct Mar.* 2023;278. <https://doi.org/10.1016/j.engstruct.2022.115565>.
- [9] Mousavi AA, Zhang C, Masri SF, Gholipour G. Damage detection and localization of a steel truss bridge model subjected to impact and white noise excitations using empirical wavelet transform neural network approach. *Meas (Lond)* Nov. 2021; 185. <https://doi.org/10.1016/j.measurement.2021.110060>.
- [10] Wang T, Zhang M, Yu Q, Zhang H. Comparing the applications of EMD and EEMD on time-frequency analysis of seismic signal. *J Appl Geophy Aug.* 2012;83:29–34. <https://doi.org/10.1016/j.jappgeo.2012.05.002>.
- [11] O'Brien EJ, Malekjafarian A, González A. Application of empirical mode decomposition to drive-by bridge damage detection. *Eur J Mech, A/Solids Jan.* 2017;61:151–63. <https://doi.org/10.1016/j.euromechsol.2016.09.009>.
- [12] Z. Wu and N.E. Huang, A study of the characteristics of white noise using the empirical mode decomposition method, *Proceedings of the Royal Society A: Mathematical, Physical and Engineering Sciences*, vol. 460, no. 2046, pp. 1597–1611, Jun. 2004, doi: 10.1098/rspa.2003.1221.
- [13] Zhang Y, Lian J, Liu F. An improved filtering method based on EEMD and wavelet-threshold for modal parameter identification of hydraulic structure. *Mech Syst Signal Process* Feb. 2016;68–69:316–29. <https://doi.org/10.1016/j.ymssp.2015.06.020>.
- [14] Aied H, González A, Cantero D. Identification of sudden stiffness changes in the acceleration response of a bridge to moving loads using ensemble empirical mode decomposition. *Mech Syst Signal Process* 2016;66–67:314–38. <https://doi.org/10.1016/j.ymssp.2015.05.027>.
- [15] Z. Wu and N.E. Huang, Ensemble Empirical Mode Decomposition: A Noise Assisted Data Analysis Method. [Online]. Available: (<http://prodav.narod.ru/hht12.htm>).
- [16] Entezami A, Sharatiadhar H. Structural health monitoring by a new hybrid feature extraction and dynamic time warping methods under ambient vibration and non-stationary signals. *Meas (Lond)* Feb. 2019;134:548–68. <https://doi.org/10.1016/j.measurement.2018.10.095>.
- [17] IEEE Signal Processing Society., 2011 IEEE International Conference on Acoustics, Speech, and Signal Processing: proceedings: May 22-27, 2011 Prague Congress Center, Prague, Czech Republic. IEEE, 2011.
- [18] Xue YJ, Cao JX, Wang DX, Du HK, Yao Y. Application of the Variational-Mode Decomposition for Seismic Time-frequency Analysis. *IEEE J Sel Top Appl Earth Obs Remote Sens Aug.* 2016;9(8):3821–31. <https://doi.org/10.1109/JSTARS.2016.2529702>.
- [19] IEEE Signal Processing Society., 2011 IEEE International Conference on Acoustics, Speech, and Signal Processing: proceedings: May 22-27, 2011 Prague Congress Center, Prague, Czech Republic. IEEE, 2011.
- [20] Delgadillo RM, Casas JR. Bridge damage detection via improved completed ensemble empirical mode decomposition with adaptive noise and machine learning algorithms. *Struct Control Health Monit Aug.* 2022;29(8). <https://doi.org/10.1002/stc.2966>.
- [21] Xin Y, Hao H, Li J. Time-varying system identification by enhanced Empirical Wavelet Transform based on Synchronizing Transform. *Eng Struct Oct.* 2019; 196. <https://doi.org/10.1016/j.engstruct.2019.109313>.
- [22] Xia YX, Zhou YL. Mono-component feature extraction for condition assessment in civil structures using empirical wavelet transform. *Sens (Switz) Oct.* 2019;19(19). <https://doi.org/10.3390/s19194280>.
- [23] Dong S, Yuan M, Wang Q, Liang Z. A modified empirical wavelet transform for acoustic emission signal decomposition in structural health monitoring. *Sens (Switz)* May 2018;18(5). <https://doi.org/10.3390/s18051645>.
- [24] J. Gilles, Empirical wavelet transform, *IEEE Transactions on Signal Processing*, vol. 61, no. 16, pp. 3999–4010, 2013, doi: 10.1109/TSP.2013.2265222.
- [25] Xia YX, Zhou YL. Mono-component feature extraction for condition assessment in civil structures using empirical wavelet transform. *Sens (Switz) Oct.* 2019;19(19). <https://doi.org/10.3390/s19194280>.
- [26] Mousavi AA, Zhang C, Masri SF, Gholipour G. Damage detection and localization of a steel truss bridge model subjected to impact and white noise excitations using empirical wavelet transform neural network approach. *Meas (Lond)* Nov. 2021; 185. <https://doi.org/10.1016/j.measurement.2021.110060>.
- [27] Tang Z, Chen Z, Bao Y, Li H. Convolutional neural network-based data anomaly detection method using multiple information for structural health monitoring. *Struct Control Health Monit Jan.* 2019;26(1). <https://doi.org/10.1002/stc.2296>.

- [28] Hou R, Xia Y. Review on the New Development Of Vibration-based Damage Identification For Civil Engineering Structures: 2010–2019. Academic Press; 2021. <https://doi.org/10.1016/j.jsv.2020.115741>.
- [29] Fan Q, Chen Z, Xia Z, Zhang W. A novel structural damage detection strategy based on VMD-FastICA and ESSAWOA. *J Civ Struct Health Monit* Jan. 2023;13(1): 149–63. <https://doi.org/10.1007/s13349-022-00629-6>.
- [30] Pan H, Azimi M, Yan F, Lin Z. Time-Frequency-Based Data-Driven Structural Diagnosis and Damage Detection for Cable-Stayed Bridges. *J Bridge Eng* Jun. 2018; 23(6). [https://doi.org/10.1061/\(asce\)be.1943-5592.0001199](https://doi.org/10.1061/(asce)be.1943-5592.0001199).
- [31] Marinello G, Pastore T, Menna C, Festa P, Asprone D. Structural damage detection and localization using decision tree ensemble and vibration data. *Comput-Aided Civ Infrastruct Eng* Sep. 2021;36(9):1129–49. <https://doi.org/10.1111/mice.12633>.
- [32] Alazzawi O, Wang D. A novel structural damage identification method based on the acceleration responses under ambient vibration and an optimized deep residual algorithm. *Struct Health Monit Nov.* 2022;21(6):2587–617. <https://doi.org/10.1177/14759217211065009>.
- [33] Z. Chen, Y. Wang, J. Wu, C. Deng, and K. Hu, Sensor data-driven structural damage detection based on deep convolutional neural networks and continuous wavelet transform, 2092, doi: 10.1007/s10489-020-02092-6/Published.
- [34] Yi T-H, Yao X-J, Qu C-X, Li H-N. Clustering Number Determination for Sparse Component Analysis during Output-Only Modal Identification. *J Eng Mech* Jan. 2019;145(1). [https://doi.org/10.1061/\(asce\)em.1943-7889.0001557](https://doi.org/10.1061/(asce)em.1943-7889.0001557).
- [35] Sen D, Erazo K, Zhang W, Nagarajaiah S, Sun L. On the effectiveness of principal component analysis for decoupling structural damage and environmental effects in bridge structures. *J Sound Vib* 2019;457:280–98. <https://doi.org/10.1016/j.jsv.2019.06.003>.
- [36] Ghoulem K, Kormi T, Bel Hadj Ali N. Damage detection in nonlinear civil structures using kernel principal component analysis. *Adv Struct Eng* 2020;23(11):2414–30. <https://doi.org/10.1177/1369433220913207>.
- [37] Sun L, Shang Z, Xia Y, Bhowmick S, Nagarajaiah S. Review of bridge structural health monitoring aided by big data and artificial intelligence: from condition assessment to damage detection. *J Struct Eng* 2020;146(5). [https://doi.org/10.1061/\(asce\)st.1943-541x.0002535](https://doi.org/10.1061/(asce)st.1943-541x.0002535).
- [38] IEEE Signal Processing Society., 2011 IEEE International Conference on Acoustics, Speech, and Signal Processing: proceedings: May 22–27, 2011 Prague Congress Center, Prague, Czech Republic. IEEE, 2011.
- [39] Mousavi AA, Zhang C, Masri SF, Gholipour G. Structural damage localization and quantification based on a CEEMDAN hilbert transform neural network approach: A model steel truss bridge case study. *Sensors* 2020;20(5). <https://doi.org/10.3390/s20051271>.
- [40] Zhang S, et al. An Adaptive CEEMDAN thresholding denoising method optimized by nonlocal means algorithm. *IEEE Trans Instrum Meas* 2020;69(9):6891–903. <https://doi.org/10.1109/TIM.2020.2978570>.
- [41] Gilles J. Empirical wavelet transform. *IEEE Trans Signal Process* 2013;61(16): 3999–4010. <https://doi.org/10.1109/TSP.2013.2265222>.
- [42] Liu W, Chen W. Recent advancements in empirical wavelet transform and its applications. *IEEE Access* 2019;7:103770–80. <https://doi.org/10.1109/ACCESS.2019.2930529>.
- [43] Zhang K, Ma C, Xu Y, Chen P, Du J. Feature extraction method based on adaptive and concise empirical wavelet transform and its applications in bearing fault diagnosis. *Meas (Lond)* 2021;172. <https://doi.org/10.1016/j.measurement.2021.108976>.
- [44] Liu W, Cao S, Chen Y. Seismic time-frequency analysis via empirical wavelet transform. *IEEE Geosci Remote Sens Lett* 2016;13(1):28–32. <https://doi.org/10.1109/LGRS.2015.2493198>.
- [45] Blanchard G, Bousquet O, Zwald L. Statistical properties of kernel principal component analysis. *Mach Learn* 2007;66(2–3):259–94. <https://doi.org/10.1007/s10994-006-6895-9>.
- [46] Anowar F, Sadaoui S, Selim B. Conceptual and empirical comparison of dimensionality reduction algorithms (PCA, KPCA, LDA, MDS, SVD, LLE, ISOMAP, LE, ICA, t-SNE). Elsevier Ireland Ltd; 2021. <https://doi.org/10.1016/j.cosrev.2021.1000378>.
- [47] Lee JM, Yoo CK, Choi SW, Vanrolleghem PA, Lee IB. Nonlinear process monitoring using kernel principal component analysis. *Chem Eng Sci* 2004;59(1):223–34. <https://doi.org/10.1016/j.ces.2003.09.012>.
- [48] B. Schölkopf, A. Smola, and K.-R. Müller, Kernel Principal Component Analysis.
- [49] Wang H, Peng M jun, Yu Y, Saeed H, Hao C ming, Liu Y kuo. Fault identification and diagnosis based on KPCA and similarity clustering for nuclear power plants. *Ann Nucl Energy* Jan. 2021;150. <https://doi.org/10.1016/j.anucene.2020.107786>.
- [50] Rahim SA, Manson G. Kernel principal component analysis for structural health monitoring and damage detection of an engineering structure under operational loading variations. *J Fail Anal Prev* 2021;21(6):1981–90. <https://doi.org/10.1007/s11668-021-01260-1>.
- [51] Ghoulem K, Kormi T, Bel Hadj Ali N. Damage detection in nonlinear civil structures using kernel principal component analysis. *Adv Struct Eng* 2020;23(11):2414–30. <https://doi.org/10.1177/1369433220913207>.
- [52] Nguyen VH, Golinalva JC. Fault detection based on Kernel Principal Component Analysis. *Eng Struct* 2010;32(11):3683–91. <https://doi.org/10.1016/j.engstruct.2010.08.012>.
- [53] K.U. LEUVEN, Z-24 bridge data, (<https://bwk.kuleuven.be/bwm/z24>).
- [54] Bisheh HB, Amiri GG. Structural damage detection based on variational mode decomposition and kernel PCA-based support vector machine. *Eng Struct* 2023; 278. <https://doi.org/10.1016/j.engstruct.2022.115565>.
- [55] Ghoulem K, Kormi T, Bel Hadj Ali N. Damage detection in nonlinear civil structures using kernel principal component analysis. *Adv Struct Eng* 2020;23(11):2414–30. <https://doi.org/10.1177/1369433220913207>.
- [56] Rahim SA, Manson G. Kernel principal component analysis for structural health monitoring and damage detection of an engineering structure under operational loading variations. *J Fail Anal Prev* 2021;21(6):1981–90. <https://doi.org/10.1007/s11668-021-01260-1>.
- [57] Mousavi AA, Zhang C, Masri SF, Gholipour G. Damage detection and localization of a steel truss bridge model subjected to impact and white noise excitations using empirical wavelet transform neural network approach. *Meas (Lond)* Nov. 2021; 185. <https://doi.org/10.1016/j.measurement.2021.110060>.
- [58] Aashto, AASHTO LRFD Bridge Design Specifications, 9th Edition - 2021 Errata. [Online]. Available: (<https://downloads.transportation.org/LRFDBDS-9-Errata.pdf>).
- [59] 318-19 Building Code Requirements for Structural Concrete and Commentary. American Concrete Institute, 2019. doi: 10.14359/51716937.